aerospace

MDPI

Article

Tactical Coordination-Based Decision Making for Unmanned Combat Aerial Vehicles Maneuvering in Within-Visual-Range Air Combat

Yidong Liu, Dali Ding *, Mulai Tan, Yuequn Luo, Ning Li and Huan Zhou

Aviation Engineering School, Air Force Engineering University, Xi'an 710038, China; lyd19981205@163.com (Y.L.); kgdtml@163.com (M.T.); 13014106881@163.com (Y.L.); lyzh_ln@126.com (N.L.); kgy_zhouh@163.com (H.Z.)
* Correspondence: kgdddl@sina.com

Abstract: Targeting the autonomous decision-making problem of unmanned combat aerial vehicles (UCAVs) in a two-versus-one (2v1) within-visual-range (WVR) air combat scenario, this paper proposes a maneuver decision-making method based on tactical coordination. First, a coordinated situation assessment model is designed, which subdivides the air combat situation into optimization-driven and tactical coordinated situations. The former combines missile attack zone calculation and trajectory prediction to optimize the control quantity of a single aircraft, while the latter uses fuzzy logic to analyze the overall situation of the three aircraft to drive tactical selection. Second, a decision-making model based on a hierarchical expert system is constructed, establishing a hierarchical decision-making framework with a UCAV-coordinated combat knowledge base. The coordinated situation assessment results are used to match corresponding tactics and maneuver control quantities. Finally, an improved particle swarm optimization algorithm (I-PSO) is proposed, which enhances the optimization ability and real-time performance through the design of local social factor iterative components and adaptive adjustment of inertia weights. Air combat simulations in four different scenarios verify the effectiveness and superiority of the proposed decision-making method. The results show that the method can achieve autonomous decision making in dynamic air combat. Compared with decision-making methods based on optimization algorithms and differential games, the win rate is increased by about 17% and 18%, respectively, and the single-step decision-making time is less than 0.02 s, demonstrating high real-time performance and win rate. This research provides new ideas and methods for the autonomous decision making of UCAVs in complex air combat scenarios.

Keywords: UCAVs; two-versus-one within-visual-range air combat; tactical coordination; expert system; maneuver decision making

check for updates

Academic Editor: Alexandre Brandão

Received: 9 January 2025
Revised: 22 February 2025
Accepted: 25 February 2025
Published: 27 February 2025

Citation: Liu, Y.; Ding, D.; Tan, M.; Luo, Y.; Li, N.; Zhou, H. Tactical Coordination-Based Decision Making for Unmanned Combat Aerial Vehicles Maneuvering in Within-Visual-Range Air Combat. *Aerospace* **2025**, *12*, 193. https://doi.org/10.3390/aerospace12030193

Copyright: © 2025 by the authors. Licensee MDPI, Basel, Switzerland. This article is an open access article distributed under the terms and conditions of the Creative Commons Attribution (CC BY) license (https://creativecommons.org/licenses/by/4.0/).

1. Introduction

In modern warfare, the contest for air supremacy has always been a key determinant of the outcome of a war. With the evolution of warfare styles brought about by advancements in technology, unmanned combat aerial vehicles (UCAVs) are playing an increasingly important role on today's battlefield [1]. The fixed-wing UCAVs (The UCAVs mentioned in this article are all fixed-wing UCAVs) have been frequently used in long-endurance reconnaissance, precision ground strikes, and support for manned aircraft operations, making them a focal point in the current military field [2]. At the current stage, the development and use of UCAVs by various countries are no longer limited to merely

serving as auxiliary equipment. Autonomous and intelligent air combat led and executed by UCAVs is an important form of future warfare [3]. Therefore, research on autonomous decision-making technology for UCAVs, which is one of the key technologies for unmanned air combat, is essential. Current research on autonomous decision-making technology mainly focuses on 1v1 air combat scenarios, but real war scenarios will not be limited to 1v1 air combat [4]. Thus, autonomous decision making for coordinated air combat by UCAVs is a problem worthy of in-depth research.

1.1. Related Work

This paper focuses on the 2v1 air combat scenario (two UCAVs on one side and an enemy aircraft on the other), specifically on how UCAVs can achieve collaborative autonomous decision making to create a synergistic effect greater than the sum of their parts. Many scholars have conducted research on autonomous aerial combat maneuver decision making, which can be mainly divided into three categories: game theory-based methods, optimization theory-based methods, and data-driven methods [5].

Game theory-based methods include differential game methods, matrix game methods [6], and influence diagram methods. Raivio proposed a game theory method for calculating the capture set of medium-range air-to-air missiles using an auxiliary degree game to replace the original complex model for trajectory identification, avoiding the complex conditions of the original problem [7]. Ref. [8] utilized air combat situation information and timeliness information to propose a constrained strategy game method, constructing a decision-making model for UCAV swarms in complex air combat environments and proposed a constrained strategy game algorithm based on linear programming and linear inequalities to solve the model. However, in high-intensity real air combat, the large computational load of this method cannot meet the real-time requirements, especially when the number of UCAVs is large. Park et al. [9] developed an automated generation algorithm based on differential game theory for UCAV visual-range air combat. This method used the relative situation in air combat to construct a scoring function matrix, transforming the optimal strategy solution into a nonlinear programming problem and using a semi-direct method to solve the adversarial strategy. These methods are well adapted to simple air combat scenarios and can quickly solve optimal maneuver decision making [10], but in real complex air combat, with the increase in participants and the evolution of the situation, the computational load becomes enormous, making it difficult to meet real-time requirements.

Optimization theory-based methods mainly include genetic algorithm-based methods, approximate dynamic programming-based methods, and other intelligent optimization algorithms [11,12]. The famous ALPHA air combat system was developed based on the genetic algorithm [13]. To reduce computation time and improve decision making efficiency, the ALPHA air combat system combined the genetic algorithm with multiple fuzzy interaction systems through the construction of a genetic fuzzy tree, compressing the solution space and decomposing a complex air combat task into multiple simple subtasks [14]. Ref. [15] adopted the idea of approximate dynamic programming, mapping the decided adversarial trajectory to the seven basic maneuver action libraries proposed by NASA. To solve the dimensionality explosion problem in air combat, the method was implemented in the air combat simulation environment through feature selection, trajectory sampling, and function approximation, ensuring real-time performance. However, the limitations of the action library still have a significant gap compared to the continuous maneuvers in reality. Tan et al. proposed a maneuver decision-making method combining an expert system with a differential evolution algorithm. First, the expert system knowledge base was used to narrow the maneuver decision-making space, and then an improved differential evolution algorithm was used to further search for the optimal control quantity,

enhancing the optimization capability. However, there is a defect of easily falling into the local optimum [16].

Data-driven methods mainly include Bayesian network-based methods, expert system-based methods, neural network-based methods, and reinforcement learning-based methods [17–20]. Meng et al. proposed a tactical recognition method based on dynamic Bayesian networks and parameter learning using the expectation-maximization parameter learning method to optimize network parameters and an autoregressive model to patch missing target information, achieving collaborative tactical recognition for beyond-visual-range (BVR) air combat between two aircraft under incomplete information [21]. Xing et al. proposed a self-organizing attack and defense adversarial decision-making algorithm using a distributed architecture where each UCAV exchanges information to select corresponding behavior rules for itself. However, this framework lacks a generalization ability for air combat scenarios [22]. Ref. [23] designed 36 basic maneuvers for offline training using the current situation and control quantity as inputs and the next situation as the output to train a neural network prediction model. However, this model requires a large number of samples for training and lacks interpretability. Refs. [24,25] both studied the application of multi-agent reinforcement learning algorithms in UCAV swarm combat and discussed the complexity of multi-agent reinforcement learning algorithms, including dimensionality explosion, difficulty in determining target rewards, environmental instability, and the balance between exploration and exploitation. However, the defect of multi-agent reinforcement learning algorithms is that they cannot encourage agents to explore new strategies and respond in unfamiliar situations. Agents can only respond to situations in the training samples or similar events. In addition, since the state space of both sides in air combat is large, exceeding 20 dimensions, obtaining samples covering the entire state space is also a challenge.

1.2. Challenges

The aforementioned research has made significant progress, but most of it focuses on 1v1 air combat scenarios and cannot cover actual application scenarios. Among the few studies on multi-UCAV combat, the research logic is roughly divided into two types. The first type is to decompose multi-versus-multi or multi-versus-one air combat into several 1v1 air combats for evaluation and decision making [26]. This only achieves a numerical overlay without involving essential differences. The second type is to assign fixed roles to each UCAV, such as the leader being responsible for offense and the wingman being responsible for luring [27,28]. This design initially applied the concept of coordinated air combat, but it is not flexible enough. Unlike the above autonomous air combat research, this study aims to design an air combat decision-making framework with coordinated situation assessment and coordinated maneuver decision-making capabilities that meets real-time requirements. For the considered scenarios, the main challenges may come from three aspects:

- Coordinated situation assessment: The UCAV formation should be assessed as a whole, and this assessment should run through the entire process of air combat. This means that a new situation assessment model needs to be designed to support maneuver decision making.
- Expert system: The design of the expert system's rules is a difficult task. First, it requires a background in air combat knowledge and cannot be detached from reality. Second, it needs to be as comprehensive as possible, covering all scenarios without conflicts between rules.
- Real-time decision-making performance: The changes in air combat situations are drastic, and the speed of decision making can largely determine victory or defeat

in battle. Therefore, the final designed decision-making algorithm must have high real-time performance.

1.3. Main Contributions

The main contribution of this paper lies in addressing the aforementioned challenges by proposing a tactical coordination-based maneuver decision-making method for UCAVs in a 2v1 WVR air combat scenario. Compared to previous work, the main contributions of this study are three aspects:

- A coordinated situational assessment model: This model divides the situational assessment of UCAVs during air combat into two categories: optimization-driven situational assessment and tactical coordinated situational assessment. Compared to traditional situational assessment models, the proposed model adds a tactical coordinated situational assessment component [29,30]. First, the tactical coordinated situational assessment provides reference values for six decision variables. Then, it determines the tactics the two-aircraft formation should adopt in the next decision cycle. Finally, the optimization-driven situational assessment provides the necessary information support for the UCAV executing the specific tactics to make maneuver decisions.
- A hierarchical expert system-based decision-making method: This method establishes a UCAV coordinated combat knowledge base containing two major categories, six decision variables, 25 rules, and 11 tactics. Compared to Ref. [16], which only has four decision variables and 11 maneuver actions as outputs, the knowledge base established in this paper is more comprehensive. It outputs tactics rather than maneuver actions, providing stronger generalization capabilities and avoiding control variable mutations caused by switching between different maneuver actions.
- An I-PSO algorithm: By designing a local social factor iteration component and adaptive adjustment of inertia weight, the optimization capability is effectively improved, and the problem of the PSO algorithm easily falling into local optima is solved.

The rest of this paper is organized as follows. Section 2 gives the air combat scenario description, air combat maneuver decision process, UCAV dynamic model, and enemy aircraft position prediction model. Section 3 presents the UCAV coordinated air combat situation assessment model. Section 4 gives the maneuver decision-making model based on the expert system. Section 5 gives the simulation results. Section 6 draws conclusions.

2. Air Combat Decision Making Problem Statement

2.1. Air Combat Scenario

In modern warfare, air operations are in most cases cluster operations, in which the two-aircraft formation is an important basic combat unit. In manned aircraft formation or manned/unmanned aircraft formation, the roles of leader and wingman are relatively fixed due to the limitation of equipment performance and pilot capability. UCAV formation, on the other hand, is not restricted, so its mode of operation is more flexible and changeable.

In the study of this paper, the air combat scenario is a 2v1 WVR air combat. Since information perception is not the focus of this paper, for the convenience of the study we assume that the position, speed, and other situational information of both sides are transparently transmitted to each other. The air combat scenario is shown in Figure 1, in which the blue aircraft represents the enemy aircraft. After acquiring our situation information, the enemy aircraft makes maneuvering decisions in accordance with the principle of avoiding falling into our missile attack zone as much as possible and aiming to form attack conditions on any one of our UCAVs. The red aircraft represents our aircraft. After acquiring the enemy aircraft's situation information, our aircraft selects the tactics to be executed according to the situation assessment in order to achieve the goal of meeting

the launch conditions against the enemy aircraft without damage. Meeting the launch condition means using the WVR infrared missile as the airborne weapon. The fire control module solves the missile attack zone in real time according to the situation of both sides, and the aircraft makes the enemy stay within the attack zone for a sustained period of time through maneuvering.

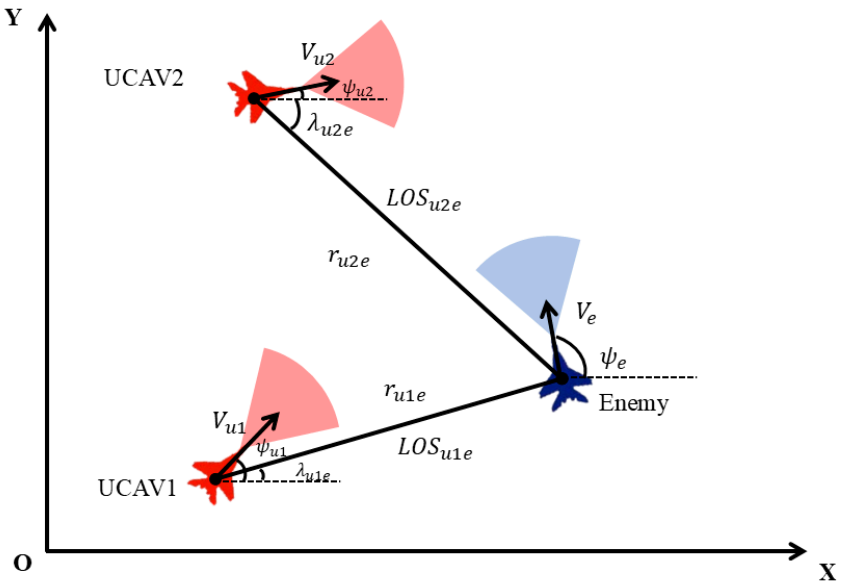

Figure 1. Horizontal air combat situation.

2.2. Air Combat Maneuver Decision-Making Process

The block diagram of the UCAV air combat maneuvering decision-making model established in this paper is shown in Figure 2. UCAVs acquire the state information of its own and the enemy's aircraft through sensors in real time, match the corresponding tactics from the knowledge library of the expert system according to the results of the tactical coordinated situation assessment and obtain the adaptive decision-making objective function factor through the real-time solving of the infrared missile attack area. After that, the trajectory prediction of the enemy aircraft is carried out, and the optimization-driven situation assessment is carried out using the prediction results to improve the decision margin. Finally, the above results are combined to plan the trajectory of each UCAV and solve the corresponding optimal control quantity, which is then sent to the flight control computer to control the UCAV to perform the corresponding maneuvers, and the above steps are repeated until the air battle is won.

Compared with Ref. [26], the decision-making method proposed in this paper has the greatest advantage in tactics, which can better reflect the coordination of formation combat. The 2v1 air battle maneuver decision in Ref. [26] is equivalent to two 1v1 air battles, in which the two UCAVs optimize their decision making by obtaining the maximum situation relative to the enemy aircraft. Such decision-making behavior is the most efficient from the perspective of pure attack, but it is also easier for the enemy aircraft to attack one of the UCAVs with a poorer situation and achieve the same result. In the same scenario, the method proposed in this paper can drive one UCAV to attack and the other to feint or lure, thus obtaining a more efficient cost ratio.

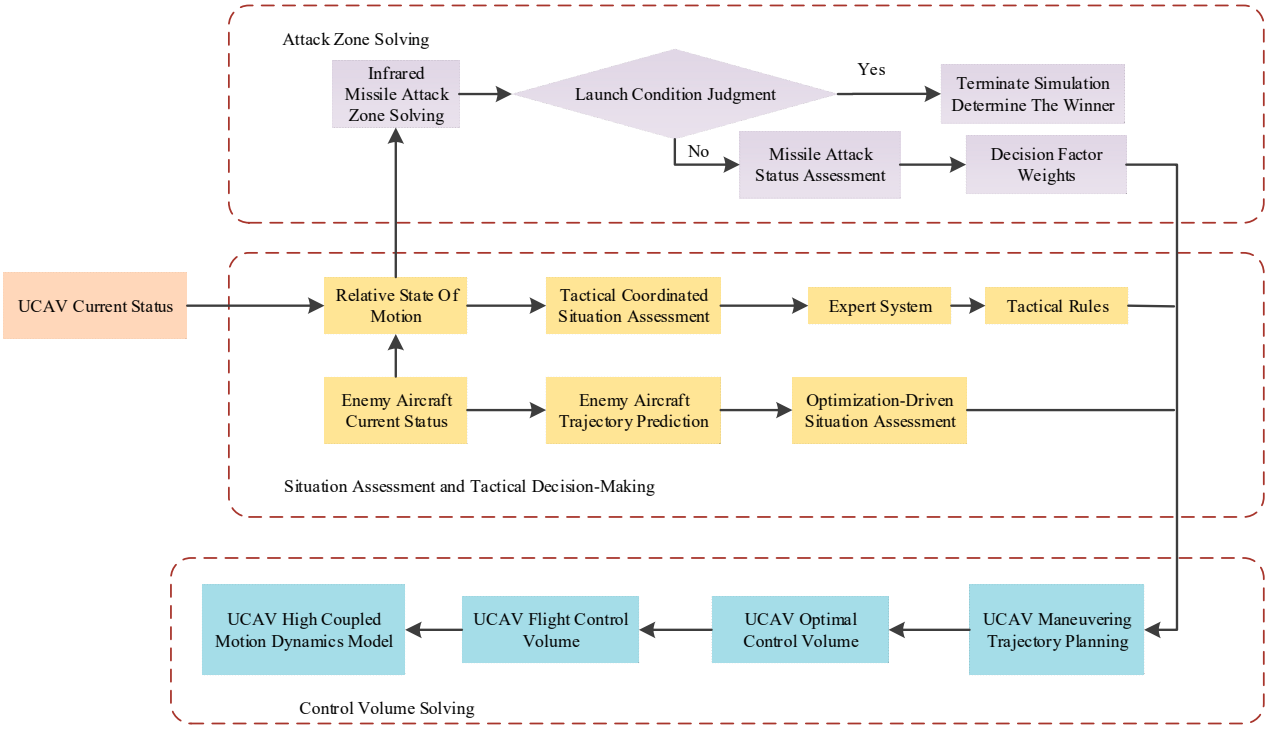

Figure 2. Block diagram of the UCAV air combat maneuver decision-making model.

2.3. UCAV Motion Dynamics Model

In order to ensure the authenticity of the research, this paper constructs a five-degrees-of-freedom aircraft model as the motion dynamics model of UCAV in the research process and uses the relevant parameters and aerodynamic data of the F-4 aircraft in the model [31]. The specific model expressions are as follows:

$$\begin{cases} \dot{x} = V \cdot \cos\gamma \cdot \cos\psi \\ \dot{y} = V \cdot \cos\gamma \cdot \sin\psi \\ \dot{z} = V \cdot \sin\gamma \\ \dot{V} = \frac{T \cdot \cos\alpha - D}{m} - g \cdot \sin\gamma \\ \dot{\gamma} = \frac{(L + T \cdot \sin\alpha) \cdot \cos\varphi}{m \cdot V} - \frac{g}{V} \cdot \cos\gamma \\ \dot{\psi} = \frac{(L + T \cdot \sin\alpha) \cdot \sin\varphi}{m \cdot V \cdot \cos\gamma} \\ L = 0.5\rho V^2 s c_l \\ D = 0.5\rho V^2 s c_d \\ T = \delta \cdot T_{\max} \\ \dot{m} = -ct \end{cases} \tag{1}$$

where $[x, y, z]$ denotes the coordinates of the UCAV in the inertial coordinate system. γ denotes the trajectory inclination of the UCAV, and ψ denotes the trajectory declination. V denotes the velocity, and m denotes the mass. g is the gravitational acceleration, and L, D, T denote the lift, air resistance, and engine thrust of the UCAV, respectively. $\rho = 1.225e^{-\frac{z}{9300}}$ denotes the air density, and S is the reference cross-sectional area of the UCAV. c_l, c_d denote the lift coefficient and drag coefficient, respectively. $c = 6.377551 \times 10^{-6}$ is the fuel consumption coefficient, and $T_{\max}$ is the maximum engine thrust.

The control quantities used in this model are $[\delta, \alpha, \varphi]$, denoting the throttle stick position, angle of attack, and trajectory roll angle, respectively. Compared to the three-degrees-of-freedom model used in reference [32], which uses tangential overload, normal

overload, and roll angle as the control quantities $[n_x, n_y, \gamma]$ of UCAV, the first is closer to the pilot's control of the airplane and is a more bottom-level control input compared to the overload model. Moreover, the three-degrees-of-freedom model does not take into account factors such as thrust, lift, and drag, and it is not realistic. In addition, in order to ensure the reliability and authenticity of the UCAV flight process, the following limitations on the minimum flight altitude and the amount of control of the UCAV are made with reference to relevant data and the literature:

$$\begin{cases} z \geq 1000 \\ -10^\circ \leq \alpha \leq 30^\circ \\ -90^\circ \leq \varphi \leq 90^\circ \\ 0.15 \leq \delta \leq 1 \end{cases} \tag{2}$$

2.4. Trajectory Prediction Model

In the process of air combat, the battlefield situation changes rapidly, and predicting the next position of the enemy aircraft can help our aircraft to form an advantageous position and achieve the launch conditions. Thus, a trajectory prediction method with a simple model and strong real-time performance is crucial. There are two main types of methods for trajectory prediction: one constructs models with a priori empirical knowledge, called the model-driven class of methods [33], and the other is a data fitting method with historical information data, called the data-driven class of methods [34]. The latter does not need to build an accurate motion model for the target and has high real-time prediction, but it requires a large amount of data for training, has high requirements for data rationality, and has poor generalization. Therefore, this paper proposes a trajectory prediction method based on trial maneuvers using the model-driven class method based on reference [35]. The principle of this method is to take the change amount $\Delta \mathbf{u}_k = [\Delta\delta_k, \Delta\alpha_k, \Delta\varphi_k]$ of the control quantity $\mathbf{u}_k = [\delta_k, \alpha_k, \varphi_k]$ as the object and find the optimal value $\Delta \mathbf{u}_k{}^* = [\Delta\delta_k{}^*, \Delta\alpha_k{}^*, \Delta\varphi_k{}^*]$ through the trial maneuver method so that the gain in the situation assessment objective function is maximized. Then, we can get the optimal control quantity $\mathbf{u}_{k+1} = [\delta_k + \Delta\delta_k{}^*, \alpha_k + \Delta\alpha_k{}^*, \varphi_k + \Delta\varphi_k{}^*]$ of the UCAV at the next moment to solve the next UCAV flight trajectory.

To ensure that the UCAV searches for the optimal maneuvering control quantity, constructs fine control quantity changes, and avoids excessive computation affecting real-time performance, nine gradient alternatives were constructed for each control quantity within the range of allowable changes, resulting in a total of 729 trial maneuvering scenarios. The gradient changes of these three control quantity changes were set as:

$$\Delta\delta_k \in \left\{ \begin{array}{l} \Delta\delta_{k,\min}, \Delta\delta_{k,\min}/2, \Delta\delta_{k,\min}/4, \Delta\delta_{k,\min}/8, 0, \\ \Delta\delta_{k,\max}/8, \Delta\delta_{k,\max}/4, \Delta\delta_{k,\max}/2, \Delta\delta_{k,\max} \end{array} \right\} \tag{3}$$

$$\Delta\alpha_k \in \left\{ \begin{array}{l} \Delta\alpha_{k,\min}, \Delta\alpha_{k,\min}/2, \Delta\alpha_{k,\min}/4, \Delta\alpha_{k,\min}/8, 0, \\ \Delta\alpha_{k,\max}/8, \Delta\alpha_{k,\max}/4, \Delta\alpha_{k,\max}/2, \Delta\alpha_{k,\max} \end{array} \right\} \tag{4}$$

$$\Delta\varphi_k \in \left\{ \begin{array}{l} \Delta\varphi_{k,\min}, \Delta\varphi_{k,\min}/2, \Delta\varphi_{k,\min}/4, \Delta\varphi_{k,\min}/8, 0, \\ \Delta\varphi_{k,\max}/8, \Delta\varphi_{k,\max}/4, \Delta\varphi_{k,\max}/2, \Delta\varphi_{k,\max} \end{array} \right\} \tag{5}$$

3. UCAV Coordinated Situation Assessment Model

Air combat situation assessment is a prerequisite for UCAV maneuver decision making, and most of the previous studies only assessed the situation through the relative states of a single UCAV and an enemy aircraft in space, often ignoring the coupled situational relationship among three aircraft (two UCAVs and one enemy aircraft). Therefore, this

paper proposes a coordinated situation assessment model, which contains two parts: the optimization-driven situation and the tactical coordinated situation. The tactical coordinated situation assessment integrates the three aircraft for consideration, and the fuzzy variables are calculated through the relative speed, bearing, angle, and other geometric relationships among the three. The variables are inputted into the expert system and matched to get the corresponding tactics, which determines the roles and tasks to be performed by our two UCAVs in the next time period and also defines the objectives and constraints for the subsequent trajectory planning and control volume solving. The optimization-driven situation assessment uses the relative state between a single UCAV and an enemy aircraft to assess and solve the missile attack zone. In addition, a trajectory prediction module is added to predict the next enemy aircraft trajectory, which is then combined with the UCAV state quantities for the optimization-driven situation assessment. Then, the optimization objective function is designed, and finally, the optimal control quantities are solved.

3.1. Optimization-Driven Situation

The spatial relativity between a UCAV and an enemy aircraft in air combat is shown in Figure 3. *LOS* denotes the line-of-sight vector from the UCAV to the enemy aircraft. Q_u and Q_e denote the entry angle of the UCAV and the enemy aircraft, respectively. V_u and V_e denote the speed of the UCAV and the enemy aircraft, respectively. D_{ue} denotes the distance between the UCAV and the enemy aircraft. $D_{\max}$ and $D_{\min}$ denote the maximum and minimum values of the far boundary of the attack zone of the UCAV missile, respectively. The purpose of the maneuver decision is to bring the enemy aircraft within the effective killing range of the UCAV's weapon while avoiding the UCAV from being attacked by the enemy aircraft.

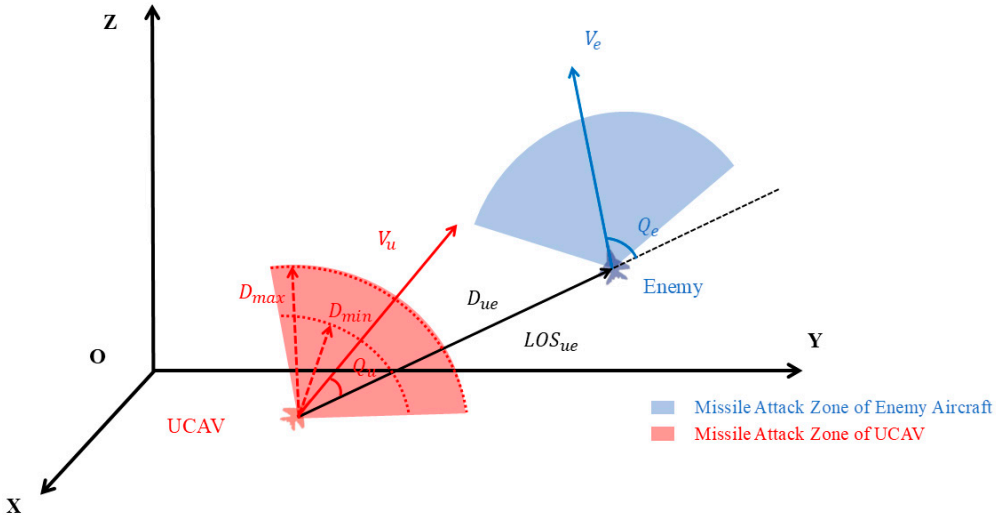

Figure 3. Schematic diagram of the air combat situation between the enemy and UCAV.

3.1.1. Azimuthal Situation Assessment Function

The position assessment function η_{A} is related to the enemy's and our advance angles Q_u and Q_{e}. From the knowledge of air combat, it is known that the smaller Q_u and Q_{e} are, the larger the azimuthal attitude η_{A} is (when $Q_u = Q_{\mathrm{e}} = 0^\circ$, $\eta_{\mathrm{Amax}} = 1$). Therefore, the expression for design η_{A} is:

$$\eta_{\mathrm{A}} = \eta_{\mathrm{A}_u} \cdot \eta_{\mathrm{A}_{\mathrm{e}}} \tag{6}$$

where η_{A_u} and η_{A_e} are expressions for assessing the azimuthal situation of the UCAV and the enemy aircraft, respectively:

$$\begin{cases} \eta_{A_u} = \frac{(sign(60^\circ \times k_a - Q_u)+1)}{2} - \frac{(sign(60^\circ \times k_a - Q_u)-1)}{2} \cdot e^{-\frac{0.5\times|60^\circ \times k_a - Q_u|}{180^\circ - 60^\circ \times k_a}} \\ \eta_{A_e} = \frac{(sign(120^\circ \times k_a - Q_e)+1)}{2} - \frac{(sign(120^\circ \times k_a - Q_e)-1)}{2} \cdot e^{-\frac{0.5\times|120^\circ \times k_a - Q_e|}{120^\circ \times k_a}} \end{cases} \tag{7}$$

where $sign(\cdot)$ is a symbolic function that takes 1, 0, or -1 depending on the input value, and it acts as a segment. The variables Q_u and Q_e in Equation (7) are calculated as follows:

$$\begin{cases} Q_u = \arccos \frac{\vec{D_{ue}} \cdot \vec{V_u}}{\left\|\vec{D_{ue}}\right\| \cdot \left\|\vec{V_u}\right\|} \\ Q_T = \arccos \frac{\vec{D_{ue}} \cdot \vec{V_e}}{\left\|\vec{D_{ue}}\right\| \cdot \left\|\vec{V_e}\right\|} \end{cases} \tag{8}$$

$$\vec{D_{ue}} = \begin{bmatrix} x_u - x_e & y_u - y_e & z_u - z_e \end{bmatrix}^T \tag{9}$$

Figure 4 gives an image of the variation of the azimuth assessment function η_A with respect to the azimuth angles Q_u and Q_e. The azimuthal situation is optimized when the enemy aircraft is located in the UCAV's attack field of view and the UCAV is outside the enemy aircraft's attack field of view, at which time $\eta_A = 1$. In the head-on or phase-off state, the two sides have an equal azimuthal situation advantage.

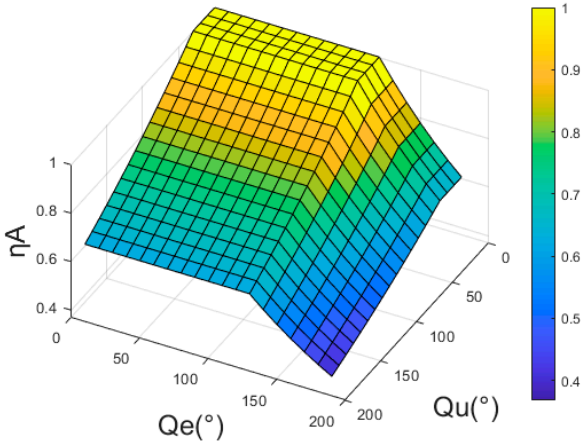

Figure 4. S Images of the variation in η_A with Q_u and Q_e.

3.1.2. Distance Situation Assessment Functions

The distance situation is assessed on the basis of the distance D_{ue} between the enemy and the distance boundary D_{max}, D_{min} of the missile attack zone. The distance situation assessment function is established based on the relative distances of the two sides:

When $Q_e \geq 120^\circ$

$$\eta_D = \begin{cases} 0, & D_{min} \leq D_{ue} \leq D_{max} \\ e^{\frac{D_{max}}{D_{max} - D_{ue}}}, & D_{ue} > D_{max} \\ e^{\frac{D_{min}}{D_{ue} - D_{min}}}, & else \end{cases} \tag{10}$$

When $Q_e < 120°$

$$\eta_D = \begin{cases} 1, & D_{\min} \le D_{ue} \le D_{\max} \\ e^{\frac{D_{\max} - D_{ue}}{D_{\max}}}, & D_{ue} > D_{\max} \\ e^{\frac{D_{ue} - D_{\min}}{D_{\min}}}, & else \end{cases} \tag{11}$$

Figure 5 gives the variation curve of the distance assessment function η_D about the distance D_{ue} between the enemy and us (the illustrated case is $D_{\max} = 5000$ m, $D_{\min} = 500$ m). When our aircraft is in the field of view of the enemy aircraft, and the distance is within the far and near boundaries of the attack zone, the distance situation is the worst, at this time $\eta_D = 0$. When the opposite is the case, the distance situation is optimal, $\eta_D = 1$.

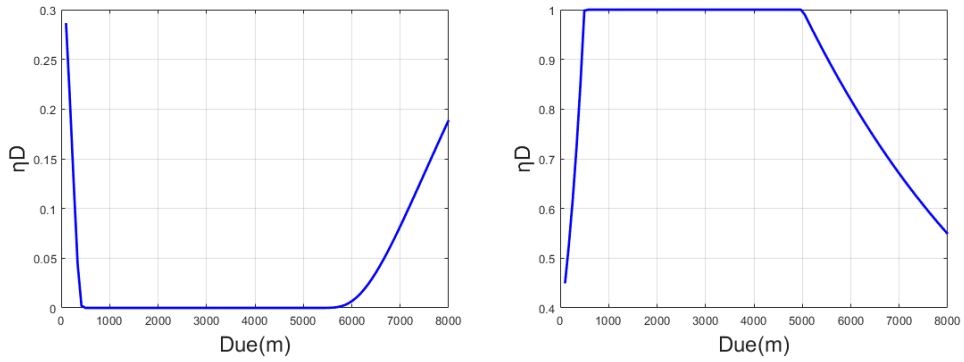

(**a**) $Q_e \ge 120°$ (**b**) $Q_e < 120°$

Figure 5. (**a**) Curve of variation of η_D with D_{ue} when $Q_e \ge 120°$; (**b**) curve of variation of η_D with D_{ue} when $Q_e < 120°$.

3.1.3. Energy Situation Assessment Function

The UCAV's energy advantage can also be viewed as a maneuver advantage, which requires the UCAV to maintain greater maneuverability relative to the enemy aircraft and is a combined representation of the UCAV's speed and altitude advantage. The energy advantage, although a smaller increase in weapon effectiveness, helps the UCAV to maintain a sustained situational advantage or to quickly escape from an unfavorable situation. Considering kinetic and potential energy per unit mass, the energy situation evaluation function η_E is expressed as:

$$\eta_E = e^{-\frac{0.5V_e^2 + g \cdot z_e}{0.5V_u^2 + g \cdot z_u + 0.5V_e^2 + g \cdot z_e}} \tag{12}$$

Figure 6 gives an image of the variation of the energy assessment function η_E with respect to the heights z_u and z_e of the UCAV and the enemy aircraft (assuming that the speeds of the two aircraft are equal, $V_u = V_e = 300$ m/s). From the figure, it can be seen that the higher the height of the UCAV relative to the enemy aircraft, the greater the energy situation.

From the above three situation assessment functions constructed, it can be seen that the situation advantage is closely related to the motion state of the UCAV relative to the target. Therefore, the single-aircraft maneuver decision is a continuous optimization process of finding the optimal control variables to obtain the maximum situation advantage.

Therefore, the computational expression for the overall optimization-driven situation of the UCAV against the enemy aircraft is:

$$\eta_u = \omega_A \cdot \eta_{Au} + \omega_D \cdot \eta_{Du} + \omega_E \cdot \eta_{Eu} \tag{13}$$

In the formula, $\omega_A, \omega_D, \omega_E$ are the weight values of different situation functions, and $\omega_A + \omega_D + \omega_E = 1$. The specific values of the three weights are calculated based on the missile attack zone solution assessment. While not repeated here, the specific method refers to Ref. [35].

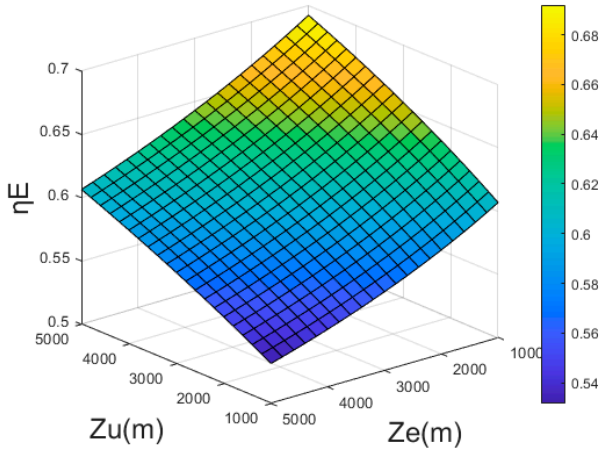

Figure 6. Images of the variation of η_E with z_u and z_e.

3.2. Tactical Coordinated Situation

The tactical coordinated situation assessment evaluates the overall situation of the formation of UCAVs relative to the enemy aircraft for the purpose of tactical decision making. Unlike the optimization-driven situation, which can accurately calculate the individual aircraft's situation value through relative state information, in order to reduce the effect of uncertainty in the acquisition of target information and at the same time achieve robust decision making, this paper utilizes fuzzy logic for the design of the tactical coordinated situation assessment function. Six fuzzy control variables are constructed, and the insensitivity of the value of the affiliation function is utilized to achieve robust decision making.

3.2.1. Relative Situation Variable

The enemy's relative situation (RS) within the line of sight is divided into active, balanced, and passive. The division of the situation is defined as follows: the angle between the two sides' velocity vectors and the target line is called the angle of advance, and when the absolute values of the angle of advance are equal, the situation is balanced. When the absolute value is smaller than that of the enemy, the situation is active, and when the absolute value is larger than that of the enemy, the situation is passive.

$$RS = \frac{|\varphi_u| - |\varphi_e|}{180^\circ} \quad RS \in [-1, 1] \tag{14}$$

where φ_u, φ_e is the advance angle and RS is a fuzzy variable taking the values of A (active), B (balance), and P (passive). The affiliation functions all use the skew-small function $A(x)$ of the ridge-shaped distribution in the F-distribution, as shown in Equation (15), and because $-180^\circ \leq \varphi_u, \varphi_e \leq 180^\circ$, the upper limit $b = 1$ and the lower limit $a = -1$ are taken.

$$A(x) = \begin{cases} 0 & b \leq x \\ \frac{1}{2} - \frac{1}{2}\sin\frac{\pi}{b-a}\left(x - \frac{a+b}{2}\right) & a \leq x < b \\ 1 & x < a \end{cases} \tag{15}$$

3.2.2. Relative Altitude Difference Variable

The difference in height (DH) takes into account the difference in height between our two aircraft and the enemy aircraft.

$$DH = (|z_e - z_{u1}| + |z_e - z_{u2}|)/1000 \quad DH \in [0, 10] \tag{16}$$

where z_e, z_{u1}, z_{u2} indicates the flight altitude and DH is a fuzzy variable taking the value of B (big), M(middle), S(small). The affiliation function uses the skew-large function $B(x)$ of the ridge-shaped distribution in the F-distribution, as shown in Equation (17). A difference in flight altitude of more than 2000 m between our aircraft and the enemy aircraft is considered to be large, so take the upper limit $b = 4$ and the lower limit $a = 0$.

$$B(x) = \begin{cases} 0 & x < a \\ \frac{1}{2} + \frac{1}{2}\sin\frac{\pi}{b-a}\left(x - \frac{a+b}{2}\right) & a \le x < b \\ 1 & b \le x \end{cases} \tag{17}$$

3.2.3. Horizontal Position Variable

Using the advance angle of the enemy aircraft relative to our aircraft, the horizontal position of the enemy aircraft relative to our formation (RPX) can be categorized into three cases, noted as $RPX = \{1, 2, 3\}$.

$RPX = 1$ indicates that the enemy plane is between the two sides of our twin planes, satisfying $45^\circ < \varphi_{e1} < 135^\circ$ and $-135^\circ < \varphi_{e2} < -45^\circ$ or $45^\circ < \varphi_{e2} < 135^\circ$ and $-135^\circ < \varphi_{e1} < -45^\circ$.

$RPX = 2$ indicates that the enemy plane is between the front and rear of our twin planes, satisfying: $|\varphi_{e1}| < 45^\circ$ and $|\varphi_{e2}| \ge 135^\circ$ or $|\varphi_{e2}| < 45^\circ$ and $|\varphi_{e1}| \ge 135^\circ$.

$RPX = 3$ indicates that the enemy aircraft is not between our two aircrafts and satisfies the other positional relationships.

3.2.4. Vertical Position Variable

Considering the relationship between the flight altitudes of our twin aircrafts and the enemy aircraft, the vertical position (RPY) of the enemy aircraft relative to our formation can be categorized into two scenarios, denoted as $RPY = \{1, 2\}$.

$RPY = 1$ indicates that the enemy plane is between the top and bottom of our twin planes, satisfying $\min(z_{u1}, z_{u2}) < z_e < \max(z_{u1}, z_{u2})$.

$RPY = 2$ indicates that the enemy plane is not between the top and bottom of our twin planes, satisfying $z_e < \min(z_{u1}, z_{u2})$ or $z_e > \max(z_{u1}, z_{u2})$.

3.2.5. Enemy Aircraft Altitude Variable

The flight altitude HE of an enemy aircraft can be expressed by the following equation:

$$HE = z_E/1000 \quad HE \in (0, 15) \tag{18}$$

where z_E is the flight altitude of the enemy aircraft in meters.

The fuzzy linguistic variables of HE take the values of H (high), M (middle), and L (low). The affiliation functions all use the skew-large function $B(x)$ of the ridge-shaped distribution in the F-distribution, as shown in Equation (17). Since below 1000 m is considered low flight, and above 10,000 m is considered high flight, the upper limit $b = 10$ and the lower limit $a = 1$ can be taken.

3.2.6. Relative Velocity Difference Variable

The relative speed difference RV is the speed difference of the enemy aircraft relative to our formation and can be expressed by the following formula:

$$RV = [2v_e \times \cos q_e \times \cos \psi_e - v_{u1} \times \cos q_{u1} \times \cos \psi_{u1} - v_{u2} \times \cos q_{u2} \times \cos \psi_{u2}]/200 \quad (19)$$

where ψ is the heading angle in degrees, indicating the angle at which the north end of the longitude line where the airplane is located turns clockwise toward our longitudinal axis, $0 \leq \psi < 360^\circ$.

q is the angle of entry, in degrees, indicating the angle between the airplane's heading and the visual line of sight and its extension, with right deviation specified as positive and left deviation as negative, $0 \leq q \leq 180^\circ$.

The fuzzy linguistic variables of RV take the values of B (big), M (middle), and S (small), which indicate large, moderate, and small relative speeds of the enemy and us, respectively. Affiliation functions all use the skew-large function $B(x)$ of the ridge-shaped distribution in the F-distribution, as shown in Equation (17).

4. Maneuvering Decision Making Based on a Hierarchical Expert System

4.1. Expert System Construction

The essence of an expert system is a rule, which is a mapping of conditions → results. The more complex the system, the more types of inputs and outputs it has. For the complex event of close air combat, the conditions and results are theoretically continuous, which means that if the inputs and outputs are discretized, it will be infinite. In order to solve this problem and thus build a reliable expert system, one feasible method is to refine the expert system by learning and summarizing a large amount of prior knowledge, but this is currently difficult to achieve for the field of air warfare, so another method is to perform fuzzification. This paper adopts the second method. Firstly, a large amount of discrete air combat situation information is converted into the readable conditions of the expert system after fuzzy reasoning, and then tactical commands are outputted through corresponding rules to finalize the tactical decision making.

4.1.1. Hierarchical Expert System Framework

There are three common types of expert system: model-based expert system, framework-based expert system, and rule-based expert system [16]. The rule representation method, also known as the if–then rule method, is a commonly used knowledge representation method in expert systems. Based on this method, we propose a hierarchical expert system decision-making framework, which is divided into two layers. The first layer is the situation information processing layer, which employs fuzzy inference to extract expert system-readable information from observation $o(t)$ and its condition $c(t)$:

$$c(t) = f(o(t)) \quad c(t) \in C \quad (20)$$

where t denotes the moment, C is a predefined set of conditions in the expert system, and $f(\cdot)$ is a mapping that processes $o(t)$ and matches $c(t)$.

The second layer is the tactical decision layer, which automatically searches and matches the output tactic tac_i when condition $c(t)$ is input and outputs maneuver control commands based on the current situation:

$$(u_i(t+1), tac_i) = h(u_i(t), c(t)) \quad tac_i \in T \quad (21)$$

where $u_i(t+1)$ denotes the control command of the ith UCAV at the moment A, including throttle stick position, angle of attack, and trajectory roll angle; tac_i denotes the tactic to be executed by the ith UCAV; and $h(\cdot)$ is a mapping between matching tac_i and computing $u_i(t+1)$.

The hierarchical expert system is the core of the UCAVs' coordinated air combat maneuver decision making, which can transform the received situation information into control commands and decide what each UCAV will do and where it will go next. Based on the idea of coordination and tactics, UCAVs are transformed into a highly coupled tactical collective, which has achieved combat effectiveness beyond the individual fighting. The pseudo-code of the decision-making algorithm is shown in Algorithm 1. It is worth noting that, to ensure the coherence of tactics, a tactical timing mechanism has been implemented. Specifically, when a tactic is determined, it will be executed for more than 5 s before the system assesses the next tactical choice. Furthermore, in the case where none of the tactical rules match, the decision-making system will guide both UCAVs to perform maneuvers to seize attack positions, with the situational function serving as the optimization objective.

Algorithm 1: Hierarchical expert system decision algorithm

Input: UCAVs and the enemy aircraft's current momentary state quantity $state(k)|_{u1,u2,e} = [x_0, y_0, z_0, v_0, \gamma_0, \psi_0, m_0]|_{u1,u2,e}$ and the current control quantity $u(k)|_{u1,u2,e} = [\delta_k, \alpha_k, \varphi_k]|_{u1,u2,e}$.
Situation Judgment: Calculation of relative situation variables $RS = \frac{|\varphi_u|-|\varphi_e|}{180^\circ}$.
if $RS_1 = P$ and $RS_2 = P$ **then**
    $tacflag = 1$ (coordinated attack tactics)
else
    $tacflag = 2$ (coordinated defensive counter-attack tactics)
end if
Selection of Tactics:
switch $tacflag$
  case 1
    calculate DH, RPX, RPY (Equations (15) and (16))
    if $RS_1 = A$ and (($RS_2 = A$ or $RS_2 = B$) and $DH = S$ and $RPX = 1$ and $tactflag = 0$ **then**
      $tactype = 2$, $tactime = 0$, $tactflag = 1$
    else if ...
    end if
  case 2
    calculate DH, RPX, RPY, HE, RV (Equations (15)–(18))
    if ...
end switch
Calculate Control Volume: According to $tactype$, designing the objective function and solving the optimal control volume by using an improved particle swarm optimization algorithm.
Output: Next moment control volume $u(k+1)|_{u1,u2,e} = [\delta_{k+1}, \alpha_{k+1}, \varphi_{k+1}]|_{u1,u2,e}$.
$tactime = tactime + 1$
if $tactime = 5$**then**
$tactflag = 0$
end if

4.1.2. Establishment of a Rule Library for an Expert System Based on a Priori Knowledge

A. Input–output fuzzification

The inputs to the fuzzy inference machine have a total of six variables: RS, DH, RPX, RPY, HE, and RV. The input variables are computed as shown in Section 3.2, along with their value ranges and affiliation functions.

The output of the fuzzy inference machine includes a total of 11 tactics with fuzzy language $[1, 2, 3, 4, 5, 6, 7, 8, 9, 10, 11]$, which represent different tactics serial numbers, and this knowledge library can be extended and improved with later learning.

B. Tactical knowledge extraction

Current approaches to maneuver decision making mostly transform the problem into a pure optimization problem with little consideration of the actual meaning behind each maneuver, which lacks interpretability and tactical significance. Therefore, this paper learns and summarizes tactical knowledge from open sources and pilots' experience sharing and transforms it into computer language.

Take the air combat tactics demonstration shown in Figure 7 as an example. At the initial moment (moment 1), both of our UCAVs are in a bad situation of being tailed, and the situation of UCAV2 is even worse, so the two planes first separate horizontally. Then, at moment 2, UCAV2 uses a decoy escape maneuver, and UCAV1 quickly turns the body direction and takes up a position to counterattack at moment 3. This paper names this tactic the horizontal defense splitting tactic.

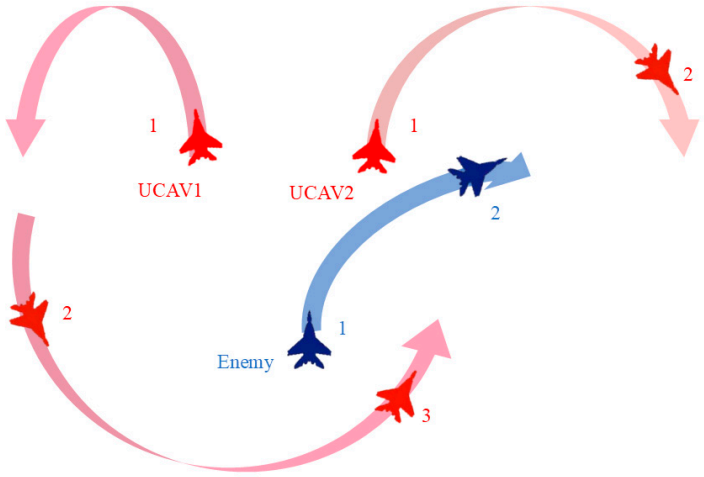

Figure 7. Demonstration of horizontal defense splitting and combining tactics.

This tactic can be extracted from the rules and is used under the following conditions: the relative situation of our aircraft is passive, the difference in altitude between the enemy aircraft and our formation is small, and the difference in relative speed is large at medium and high altitudes. Tactical behavior is described as follows: when approaching the enemy's close-range combat rounds fire range, our two planes suddenly separate horizontally, and if the enemy tracks one of our planes, the other one will quickly take up the position and then carry out a counterattack. It can be described by the if–then rule statement as follows: if $RS_1 = P$ and $RS_2 = P$ and $DH = S$ and $HE = -L$ and $RV = B$, then $tactype = 7$.

4.2. Improved Particle Swarm Optimization Algorithm

At the tactical decision-making level, control commands need to be solved after the expert system has determined the tactics to be executed in the next moment. This refines the decision problem into an optimization problem with boundary constraints, whose general form can be described in mathematical language as follows:

$$\begin{aligned} \min \quad & J(x) \\ \text{s.t.} \quad & \dot{x} = f(x,u,t) \\ & x_L \le x \le x_M \\ & u_L \le u \le u_M \end{aligned} \tag{22}$$

where $J(x)$ is the objective function and x_L, x_M, u_L, u_M are the boundary constraints.

In this paper, the classical particle swarm optimization algorithm is improved for solving optimization problems, mainly for the defect that a particle swarm algorithm can easily fall into the local optimum. Considering the drastic change in air combat situation, the real-time requirement of decision making is high, so the improvement should be carried out under the premise of avoiding increased computational complexity.

4.2.1. Principles of the PSO Algorithm

The PSO algorithm is a classic and common optimization algorithm, so only its principle is briefly explained here. The PSO algorithm is a kind of intelligent algorithm that simulates the foraging behavior of birds, and it can complete the best value optimization by following the personal best value and the group best value. The following is the formula for updating particles in the particle swarm optimization algorithm:

$$\begin{aligned} v_{k+1}^i &= \omega \cdot v_k^i + c_1 \cdot rand \cdot \left(P_{best,k}^i - X_k^i\right) + c_2 \cdot rand \cdot \left(G_{best,k} - X_k^i\right) \\ X_{k+1}^i &= X_k^i + v_{k+1}^i \cdot dt \end{aligned} \tag{23}$$

where i denotes the ith particle; k is the number of iterations; ω is the inertia weight; X denotes the position of the particle; v denotes the velocity of the particle; c_1 and c_2 denote the self-learning factor and the social learning factor, respectively; $rand$ is a random number uniformly distributed between $[0,1]$; P_{best} and G_{best} denote the personal best value and the group best value, respectively; and dt denotes the simulation interval, which can be taken to be 1 in general.

4.2.2. Improvement in Social Factor

The velocity update part of the particle swarm optimization algorithm can be considered to have three parts. The first part is the self-inertia factor iteration, which retains the previous velocity information for the next iteration. The second part is the self-optimal factor iteration; P_{best}^i is the position of the ith particle with the highest adaptive degree in all previous iterations, which can be understood as the position of the self closest to food in history. The third part is the social factor iteration, G_{best}, which is the position of the population with the highest adaptive degree in all the previous iterations. It can be understood as the nearest position of all the particles closest to the food in the history.

The social factor iteration in the third part tends to make the whole particle population approach the particle position represented by G_{best}. When G_{best} is a local optimal solution, this means that the final result of the particle swarm optimization falls into a local optimum. In order to solve this problem without additional computation, this paper improves the two parts of inertia weight ω and social factor iteration, and the improved particle velocity iteration formula is:

$$\begin{aligned} v_{k+1}^i = &\left(\omega_k - \tfrac{k}{K} \cdot \eta \cdot \omega_k\right) \cdot v_k^i + c_1 \cdot rand \cdot \left(P_{best,k}^i - X_k^i\right) + \\ &c_2 \cdot rand \cdot \left[q \cdot \left(G_{best,k} - X_k^i\right) + (1-q) \cdot \left(L_{best,k}^i - X_k^i\right)\right] \end{aligned} \tag{24}$$

where K is the maximum number of iterations; η is the attenuation coefficient; q is the scale factor with the value interval $[0,1]$; and L_{best}^i is the coordinates of the locally optimal solution of the ith particle.

Compared to the original particle swarm optimization algorithm, the improved algorithm (I-PSO) has the following two advantages:

A. Adjusting the calculation of inertia weight ω to decay as the iteration proceeds can make the value of ω change from fixed to large in the pre-iteration period and small in the later period. This can ensure that the particles are fully traversed in the early iteration as well as in the late iteration to reduce the impact of the particle's own inertia and increase the impact of the extreme value to improve the iteration speed.

B. The third part can be expanded into two parts: the local social factor iteration and global social factor iteration. The local social factor is used to increase the likelihood that the global optimum is traversed, thus eliminating the defect that the global social factor may fall into a local optimum.

First define an adjacency matrix **D**:

$$\mathbf{D} = \begin{bmatrix} d_{11} & d_{12} & \cdots & d_{1n} \\ d_{21} & d_{22} & \cdots & d_{2n} \\ \vdots & \vdots & \ddots & \vdots \\ d_{n1} & d_{n2} & \cdots & d_{nn} \end{bmatrix} \tag{25}$$

where d_{ij} represents the distance from the jth particle to the ith particle when $i = j$, $d_{ij} = 0$.

Then, define a hypersphere with a certain particle as the center and R as the radius. The neighboring particles within the hypersphere are screened by the adjacency matrix **D**. Then, the particle with the highest fitness is compared and calculated, and its position is recorded. Next, the local optimum coordinate L^i_{best} of the particle is obtained.

$$L^i_{best} = avg\left[\min\left[f\left(X^j_k\right)\right]\right], \quad \left\|X^j_k - X^i_k\right\| \le R \tag{26}$$

The pseudo-code of the I-PSO algorithm is shown in Algorithm 2.

Algorithm 2: I-PSO algorithm

Initialization: Set population size N, spatial dimensions d, maximum number of iterations K, displacement simulation intervals dt, position limits $X_{\min}, X_{\max}$.
Population Initialization: $X^i_0 = X_{\min} + rand \cdot (X_{\max} - X_{\min}), \quad i = 1, 2, \cdots N$
for $k = 0$ to K **do**
  calculate the fitness $f(X^i_k)$
  $\mathbf{D} = [d_{ij}]_{n\times n}, d_{ij} = \left\|X^j_k - X^i_k\right\|$
  $L^i_{best,k} = avg\left[\min\left[f\left(X^j_k\right)\right]\right]$
  if $k = 0$ **then**
    $P^i_{best,k} = X^i_0$
  else
    $P^i_{best,k} = avg\left[\min\left[f\left(X^i_{k-1}\right), f\left(X^i_k\right)\right]\right]$
  end if
  $G_{best,k} = avg\left[\min\left[f\left(P^i_{best,k}\right)\right]\right]$
  Update Speed: $v^i_{k+1} = \omega_k \cdot v^i_k + c_1 \cdot rand \cdot \left(P^i_{best,k} - X^i_k\right) + c_2 \cdot rand \cdot \left[q \cdot \left(G_{best,k} - X^i_k\right) + (1-q) \cdot \left(L^i_{best,k} - X^i_k\right)\right]$
  Update Location: $X^i_{k+1} = X^i_k + v^i_{k+1} \cdot dt$
  Update Inertia Weights: $\omega_{k+1} = \left(\omega_k - \frac{k}{K} \cdot \eta \cdot \omega_k\right)$
end for
Output: The optimal solution is $G_{best,K}$, the fitness is $f(G_{best,K})$.

In order to verify the optimization ability of the I-PSO algorithm, this paper compares it with the PSO algorithm and the DE algorithm [36] using the basic test function set, and the test results are shown in Figure 8. It can be seen from the three convergence graphs that the I-PSO algorithm has a better optimization-seeking ability and convergence speed.

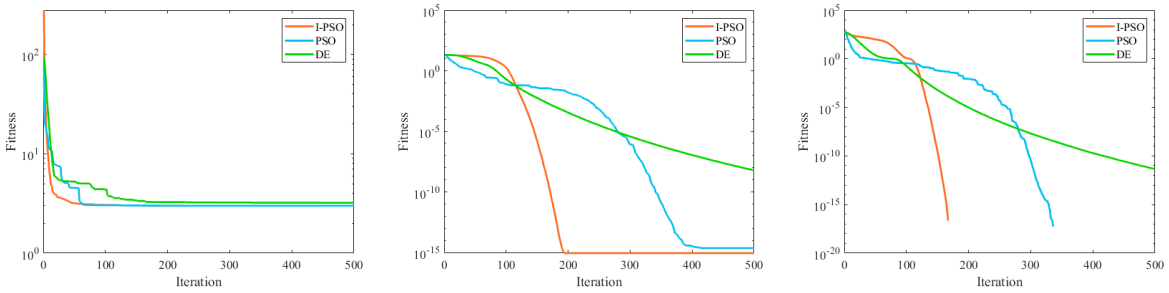

Figure 8. Convergence curves of the three algorithms: (**a**) test function 1; (**b**) test function 2; (**c**) test function 3.

5. Simulation Verification and Analysis

In order to verify the feasibility and effectiveness of the proposed method, 2v1 air combat simulations were conducted. The setup of the air combat confrontation scenario was introduced in Section 2.1. Our side uses the decision-making method proposed in this paper, and the enemy aircraft uses the test maneuver decision-making method. In order to ensure that the simulation is as close as possible to the actual, the following three rules are set:

- Win/loss conditions: If one of our two UCAVs is destroyed while the enemy is intact, the enemy will be awarded a win, and we will be awarded a loss. If the enemy's aircraft is destroyed while ours is intact, we will be awarded a win, and the enemy will be awarded a loss. If the upper limit of the simulation time is reached and both sides are intact, then a draw will be awarded.
- Aircraft destruction conditions: If the aircraft is locked by the enemy aircraft for 6 s consecutively to reach the missile launching conditions or the flight altitude is less than or equal to the minimum flight altitude, then the aircraft will be destroyed.
- Tail-behind attack: In order to achieve the attack conditions in close air combat and at the same time to ensure that they are in a safe position, the aircraft will try to choose the tail-behind attack to occupy the position.

The relevant parameter settings for the simulation experiment are shown in Table 1, and the simulation environment is Intel Core i5-12500H, 2.50 GHz, 16.0 GB RAM, MATLAB R2021b.

Table 1. Simulation parameter settings.

Parameter	Value	Unit
δ	[0.15, 1]	1
α	$[-10, 30]$	°
φ	$[-90, 90]$	°
V	[80, 600]	m/s
H	[500, 15,000]	m
ω	0.8	1
c_1	0.5	1
c_2	0.2	1
η	0.8	1
dt	1	1

In order to verify the superiority of the algorithm proposed in this paper, the simulation is set up with four different initial confrontation situations: head-on, trailing, being trailed, and parallel. The simulation experiments based on Scenario 1 were unfolded to focus on the analysis. In addition, a comparison experiment between this paper's method and the maneuver decision-making method based on the optimization algorithm was also conducted.

5.1. Scenario 1: Head-On Situation

In Scenario 1, at the initial moment, our formation is flying head-on with enemy aircraft. The initial state vectors of our two UCAVs are $S_{u1} = [10000, 2000, 7000, 250, 0, 180, 14680]$ and $S_{u2} = [9500, -1000, 9000, 250, 0, 180, 14680]$. Taking S_{u1} as an example, this vector indicates that the initial position coordinates are $[10000, 2000, 7000]$, the initial velocity is 250 m/s, the initial track inclination is 0°, the track declination is 180°, and the initial aircraft mass is 14,680 kg. The initial state vector of the enemy aircraft is $S_e = [0, 0, 8000, 250, 0, 0, 14680]$, and the simulation step is 1 s.

The entire air battle simulation lasts for 39 s. Figure 9a depicts the flight trajectories of the three aircraft, and it can be observed that despite the maneuvers taken by the enemy aircraft represented by the blue aircraft, it is still attacked by the UCAV2 to obtain the attack conditions and complete the lock. The relative situation of the two sides is shown in Figure 9c, from which it can be seen that the relative situation values are basically equal at the initial moment because both sides are in a head-on position, which is approximately equalized. At the end of the criticality, UCAV2 has already completed the tail-behind attack to occupy the position by maneuvering, and gained a higher value of the situation. Based on the decision framework proposed in this paper, our side can switch between different confrontation phases more smoothly and utilize the coordination between UCAVs.

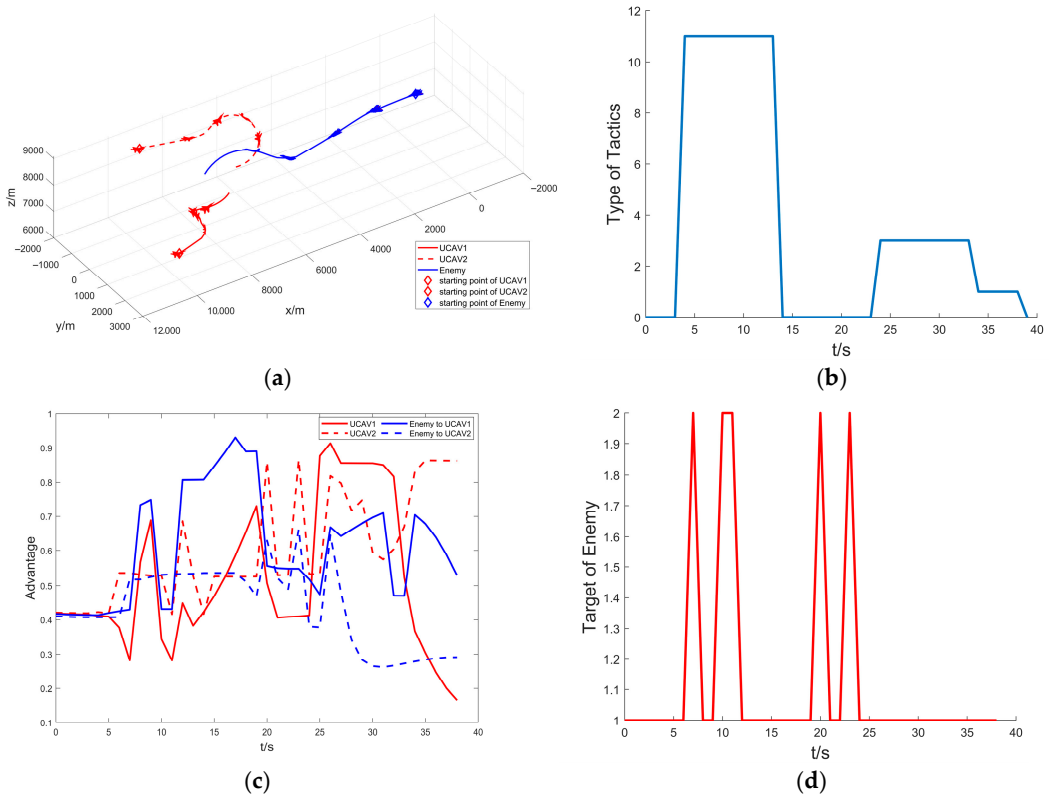

Figure 9. Simulation results for head-on situation; (**a**) trajectories of the three aircrafts; (**b**) types of tactics used by UCAVs; (**c**) change in situation value for the three aircrafts; (**d**) targeting change in enemy aircraft.

Figure 9b visualizes the tactics adopted by our formation, and different values on the vertical coordinate represent different tactics. As shown in the figure, our tactical decision-making process can be divided into five phases: approaching flight (0~4 s), bait attack (4~13 s), contract attack (14~23 s), up-down pincer attack (24~33 s), and cover attack (34~39 s).

- Approaching flight (0~4 s): We adopt an approaching strategy to rapidly close the distance in order to make the enemy fall into our attack zone (Tactic 0).
- Bait Attack (4~13 s): Since both sides are in an even position and the difference in altitude between the enemy aircraft and our two-aircraft is large, we adopt the baiting tactic. UCAV1, which has an altitude advantage, takes the role of the main attacker, while UCAV2 acts as a decoy to maneuver in a direction more favorable to UCAV1 (Tactic 11).
- Contract attack (14~23 s): At 14 s, our UCAV1 is in a disadvantageous position, and UCAV2 is in an even position, so we use the strategy of contract offense to reverse the position (Tactic 0).
- Up-down pincer attack (24~33 s): At 24 s, our two-aircraft formation is close to the enemy aircraft, and the enemy aircraft is between the top and bottom of our two-aircraft formation. Therefore, our two aircrafts turn toward the enemy planes from high altitude and low altitude at the same time and carry out a pincer attack (Tactic 3).
- Cover attack (34~39 s): At 34 s, through the aforementioned tactical maneuvers, we gain advantage of the overall situation, and the enemy aircraft enters the missile attack zone of UCAV2. Therefore, UCAV2 continues to maneuver to ensure that launch conditions are met, and UCAV1 provides cover until the enemy aircraft is destroyed, while maintaining its own safety (Tactic 1).

In summary, during the air confrontation, the tactical rules are dynamically switched according to the triggering event. The target selection of the enemy aircraft is shown in Figure 9d, and it can be seen that since UCAV1 is at an altitude disadvantage, the enemy aircraft is maneuvering with UCAV1 as the attack target most of the time. In the bait attack phase, UCAV2 acts as a decoy, causing the enemy aircraft to change its attack target, thus giving up the advantage it has. It is through tactical coordination, utilizing constant changes in roles and tactics, and sacrificing some of our advantages to neutralize the original advantages of the enemy aircraft, that we ultimately make the enemy aircraft fall into a disadvantage until they are destroyed.

5.2. Scenario 2: Trailing Situation

In Scenario 2, at the initial moment, our formation is behind the tail of the enemy aircraft. The initial state vectors of our two UCAVs are $S_{u1} = [-10000, 2000, 7000, 250, 0, 0, 14680]$ and $S_{u2} = [-9500, -1000, 9000, 250, 0, 0, 14680]$. The initial state vector of the enemy aircraft is $S_e = [0, 0, 8000, 250, 0, 0, 14680]$, and the simulation step is 1 s.

Figure 10a shows the entire air battle, which lasts 70 s. We have an initial advantage because we are behind the enemy's tail at the initial moment. The enemy's first maneuver is a diagonal rearward downward half somersault, which turns the aircraft's pointing direction in a short time to regain the situational advantage and return to a near-even situation (at 10 s). However, because such a maneuver loses some speed and altitude, as shown in Figure 10c, the enemy aircraft remains at a disadvantage in the subsequent circling entanglements.

In the phases at 10~19 s and 50~70 s, our two aircrafts use cover attack tactics. At the 20~49 s phase, our formation uses feinting and holding tactics, and the roles are switched at the 36 s. At 20~36 s, UCAV2, with a better situation, takes the role of attacking aircraft

to occupy the position, while UCAV1, with a poorer situation, feints to hold the attention of the enemy aircraft. After 36 s, UCAV1's situation is better, and it is easier for it to form a favorable condition for attacking, so it immediately switches its role from feinting to the main attacking. Finally, under the cover of UCAV2, the missile launching condition is formed, and the game is won.

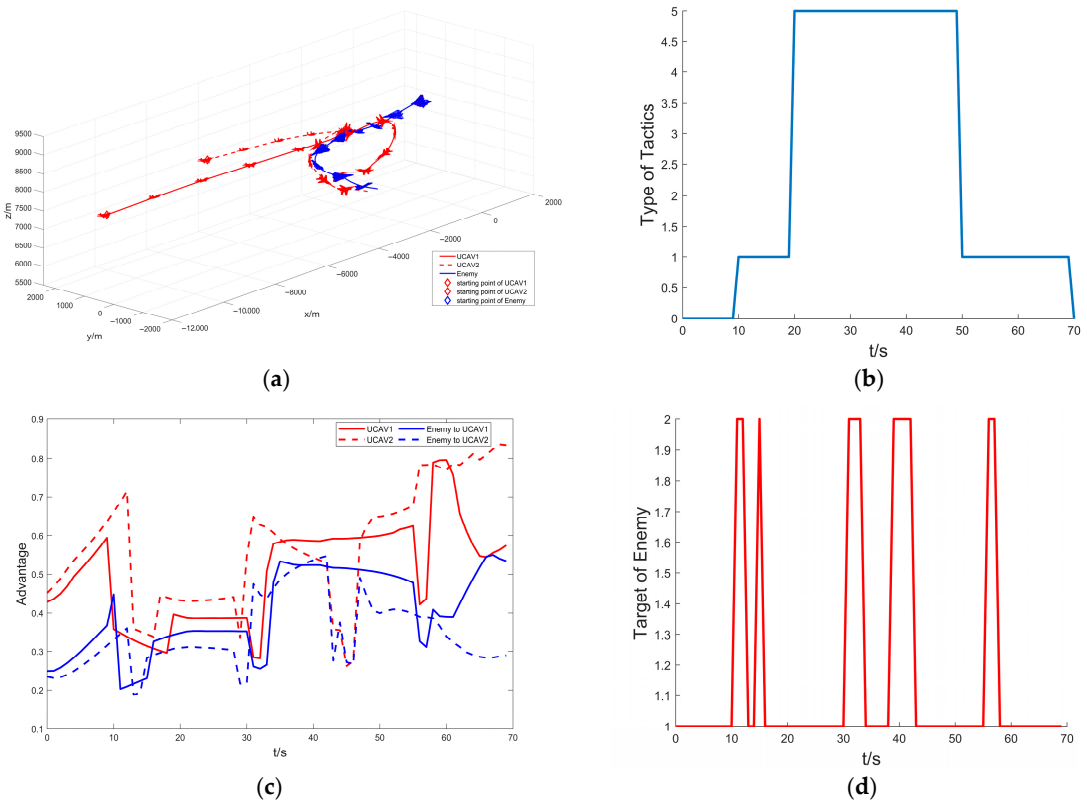

Figure 10. Simulation results for trailing situation: (**a**) trajectories of the three aircrafts; (**b**) types of tactics used by the UCAVs; (**c**) change in situation value for the three aircrafts; and (**d**) targeting change in enemy aircraft.

5.3. Scenario 3: Trailed Situation

In Scenario 3, at the initial moment, the enemy aircraft is behind our formation. The initial state vectors of our two UCAVs are $S_{u1} = [10000, 2000, 7000, 250, 0, 0, 14680]$ and $S_{u2} = [9500, -1000, 9000, 250, 0, 0, 14680]$. The initial state vector of the enemy aircraft is $S_e = [0, 0, 8000, 250, 0, 0, 14680]$, and the simulation step is 1 s.

Figure 11a shows the flight trajectories of the three aircrafts during the whole air combat process, which lasts for 98 s. At the initial moment, in order to get rid of the disadvantage of being tailed, our formation chooses to turn the flight direction by 180°. After assessing the tactical situation and matching the rules, we adopt the four tactics of bait attack (11~20 s), feint and hold (21~50 s), bait attack (51~80 s), and cover attack (91~98 s), in order.

From Figure 11c, we know that the situation of UCAV1 is extremely poor at 51~80 s. At the same time, we choose to adopt the tactic of baiting the enemy to attack. UCAV2 acts as a decoy to bait the enemy to maneuver and takes the initiative to reduce its own value in the situation in exchange for the probability of UCAV1's survival. Then, we counterattack together with our two UCAVs after they are safe.

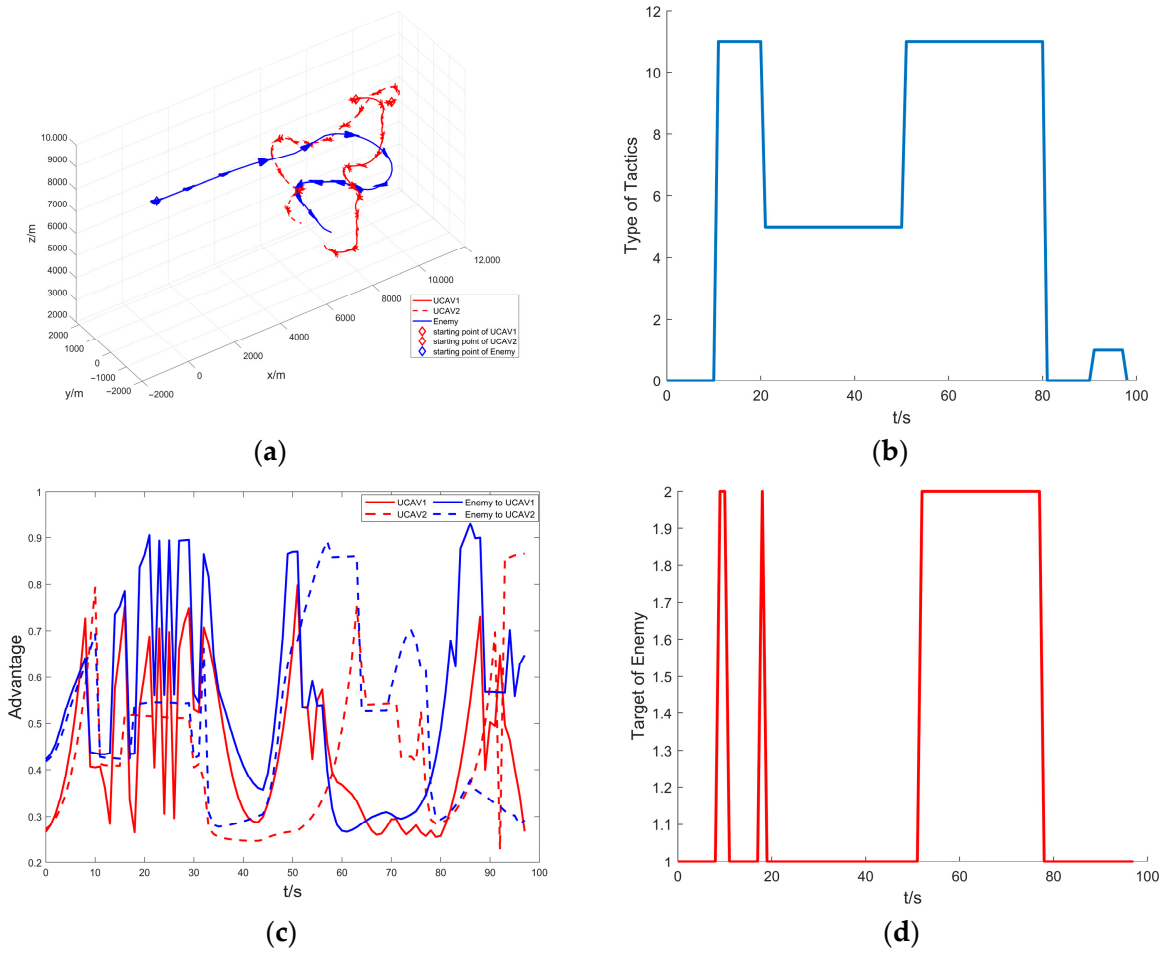

Figure 11. Simulation results for the trailed situation: (**a**) trajectories of the three aircraft; (**b**) types of tactics used by UCAVs; (**c**) change in situation values for the three aircrafts; (**d**) targeting change in enemy aircraft.

5.4. Scenario 4: Parallel Situation

In scenario 4, at the initial moment, the enemy aircraft and our formation are in a situation in which they are parallel to each other, and their speeds are in opposite directions. The initial state vectors of our two UCAVs are $S_{u1} = [0, 10000, 7000, 250, 0, 180, 14680]$ and $S_{u2} = [0, 9000, 9000, 250, 0, 180, 14680]$. The initial state vector of the enemy aircraft is $S_e = [0, 0, 8000, 250, 0, 0, 14680]$, and the simulation step is 1 s.

The results of the air combat simulation are shown in Figure 12, and the simulation conducted under Scenario 4 is the longest among the four simulations, totaling 115 s, which is determined by the initial positions of both sides. From Figure 12a, it can be seen that the two sides find each other from different initial positions and then turn to approach each other. After that, they enter the dogfight phase, and since neither side has any initial advantage, the winner could not be determined in a short period of time. From the flight trajectories, we can see that both sides perform complicated maneuvers. It is only through many tactical changes that our formation is able to achieve the launch conditions: under the cover of UCAV1, UCAV2 is able to win, which also reflects our strong decision-making ability.

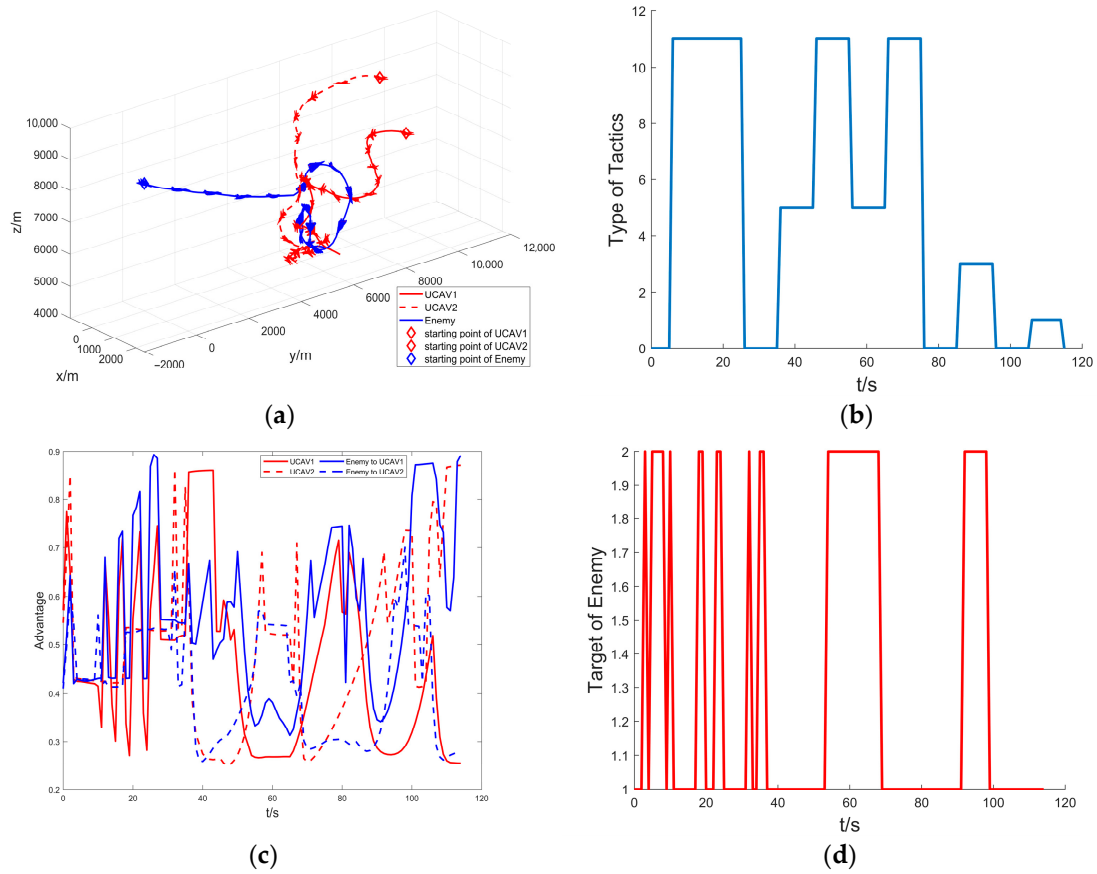

Figure 12. Simulation results for parallel situation; (**a**) trajectories of the three aircraft; (**b**) types of tactics used by UCAVs; (**c**) change in situation value for three aircraft; (**d**) targeting change of enemy aircraft.

5.5. Comparison and Analysis

In order to verify the superiority of the algorithm proposed in this paper, we compared it with the optimization algorithm-based maneuver decision-making method in a simulation. The same 2v1 air combat scenario was set up, differing only in the decision-making part. We conducted 2000 Monte Carlo experiments using the winning rate of two UCAVs as the evaluation metric (if the air combat was tied, the air combat of that game was replayed). To eliminate chance, we took the average of the results of every 10 air battles as the evaluation value, and the final results are shown in Figures 13 and 14.

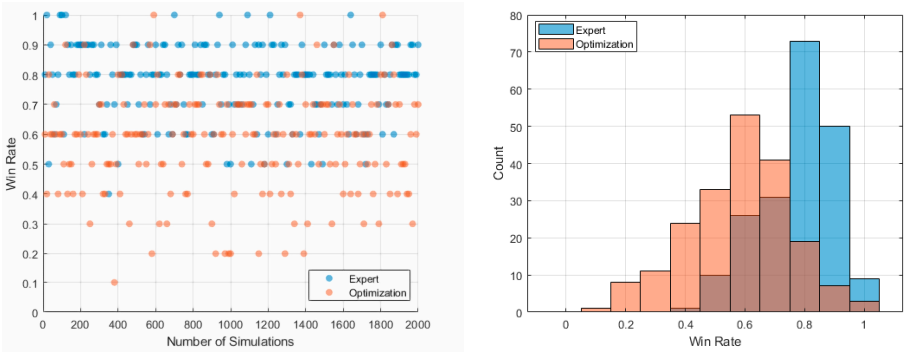

Figure 13. The win rate comparison with the method based on optimization algorithms (bigger is better): (**a**) one discrete point in the subfigure corresponds to the average win rate of 10 MC trials; (**b**) depicts the distribution of win rate.

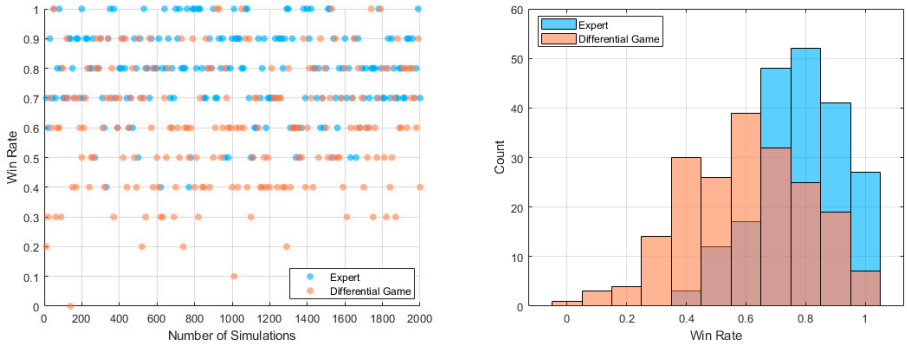

(**a**) (**b**)

Figure 14. The win rate comparison with the method based on differential game algorithms (bigger is better): (**a**) one discrete point in the subfigure corresponds to the average win rate of 10 MC trials; (**b**) depicts the distribution of the win rate.

From Figure 13, we can see that the algorithm proposed in this paper performs better, with an average of 0.7883:0.6121. This means that for every 10 air combat simulations, the formation of UCAVs using the decision-making method proposed in this paper can defeat the enemy while remaining intact about 7.9 times, compared with only 6.1 times for the UCAVs that make decisions based on the optimization algorithm. In Figure 14, the win ratio of the two methods is 0.7894:0.6065. This indicates that rapid situation assessment and reasonable tactical rule selection can effectively improve the combat capability of UCAVs.

To assess the real-time performance of the proposed decision-making method, we compared the average CPU time per step between the proposed method and the maneuver decision-making method based on optimization algorithms, as shown in Figure 15. The comparison results showed that both methods can achieve decision making at the 0.01 s level, but the method proposed in this paper seems slightly faster. Our hypothesis is that the specific state rule classification in the hierarchical expert system allows the agent to search less state space at each step, consuming less time.

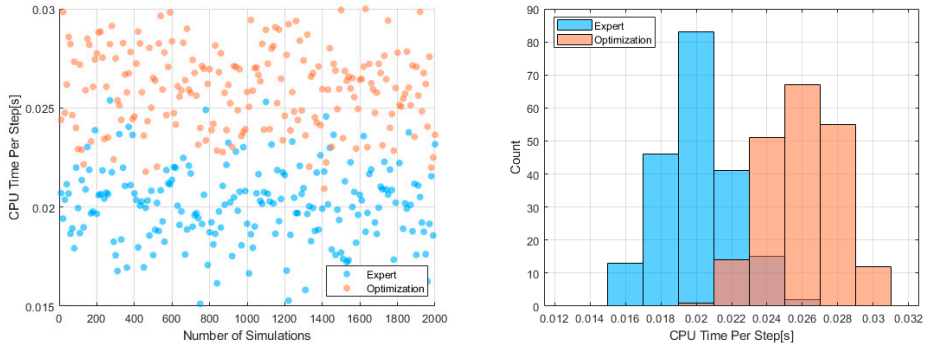

(**a**) (**b**)

Figure 15. The computational performance comparison with the method based on differential game algorithms (smaller is better): (**a**) one discrete point in the subfigure corresponds to the average CPU time of 10 MC trials; (**b**) depicts the distribution of CPU time.

5.6. Discussion

To verify the superiority and effectiveness of the proposed algorithm in this paper, this section sets up and conducts air combat simulations under four classic scenario conditions, as well as win rate and real-time performance tests with the maneuver decision-making method based on optimization algorithms. In the simulations of the four scenarios, our UCAV formation achieved stable flight trajectories and flexible tactical changes, and through the method of tactical collaboration, it expanded the advantages and reversed

the disadvantages, which strongly proved the effectiveness of this method. In addition, through the comparison tests, we can see that this method increased the win rate by about 17% compared with the maneuver decision-making method based on optimization algorithms and by about 18% compared with the maneuver decision-making method based on differential games. Moreover, with an average decision-making time of 0.02 s, it achieved stronger real-time performance. Referring to the 50 Hz data update frequency of the flight control computer, this method can fully meet the real-time requirements. In the two Monte Carlo experiments, the win rate of our method was around 79%, which also shows the stability of this method.

6. Conclusions

A tactical coordination-based UCAV maneuver decision-making method for 2v1 WVR air combat was proposed in this paper. To address the lack of consideration for coordination and tactics among UCAVs in existing decision-making algorithms, we designed two core models: a coordinated situation assessment model and a decision model based on a hierarchical expert system. The former innovatively proposes a tactical coordinated situation assessment method, which regards the three aircrafts of both sides as a whole and conducts a situation assessment from a tactical perspective. The latter constructs a hierarchical decision-making framework containing a UCAV-coordinated combat knowledge base and uses the situation assessed by the former to match and calculate corresponding tactics and maneuver control quantities. In addition, the I-PSO algorithm is proposed to improve the accuracy of algorithm decision making. Simulations conducted in multiple scenarios demonstrated that the decision-making method proposed in this paper can achieve autonomous decision making in dynamic air combat and had high real-time performance and effectiveness.

Although the method proposed in this paper achieved good performance, there are still some aspects that need to be improved in the future.

- The air combat scenario constructed in this paper is idealized and does not take into account the impacts of information transmission loss, electronic interference, and sensor inaccuracy. How to overcome these potential impacts is an important aspect to further enhance the authenticity of the research.
- The effectiveness of the method proposed in this paper largely depends on the completeness of the knowledge base. Therefore, it is necessary to further improve and expand the knowledge base to adapt to more dynamic situations.
- This paper is based on a 2v1 air combat scenario for research, while the number of aircraft in real air combat will not be limited to this. Therefore, it is necessary to consider expanding the knowledge base or combining it with target allocation algorithms to adapt to scenarios with a larger number of aircrafts.

Author Contributions: Conceptualization, Y.L. (Yidong Liu) and D.D.; methodology, Y.L. (Yidong Liu) and M.T.; software, writing—original draft preparation, Y.L. (Yidong Liu); validation, Y.L. (Yidong Liu) and Y.L. (Yuequn Luo); formal analysis, Y.L. (Yuequn Luo); data curation, N.L.; writing—review and editing, Y.L. (Yidong Liu) and D.D.; project administration, funding acquisition, D.D. and H.Z. All authors have read and agreed to the published version of the manuscript.

Funding: This work was supported by National Natural Science Foundation of China (Grant No. 62101590).

Data Availability Statement: The data used to support the findings of this study are included within the article.

Acknowledgments: I thank my teachers, friends, and other colleagues for their discussions on simulation and comments on this paper.

Conflicts of Interest: The authors declare no conflicts of interest.

References

1. Ding, D.; Xie, L.; Wang, Y. The application of manned/unmanned aerial vehicle cooperative combat and its influence on war form. *Unmmaned Syst. Technol.* **2020**, *3*, 1–9.
2. Liu, X.; Yin, Y.; Su, Y.; Ming, R. A Multi-UCAV Cooperative Decision-Making Method Based on an MAPPO Algorithm for Beyond-Visual-Range Air Combat. *Aerospace* **2022**, *9*, 563. [CrossRef]
3. Air Superiority 2030 (AS 2030) Enterprise Capability Collaboration Team. *Air Superiority 2030 Flight Plan*; United States Air Force: Washington, DC, USA, 2016.
4. Cheng, X.; Shi, W.; Cai, W.; Zhu, W.; Shen, T.; Shu, F.; Wang, J. Communication-efficient coordinated RSS-based distributed passive localization via drone cluster. *IEEE Trans. Veh. Technol.* **2021**, *71*, 1072–1076. [CrossRef]
5. Chen, H.; Huang, J.; Liu, Q.; Zhou, S.; Zhang, Z. Review and prospects of autonomous air combat maneuver decisions. *Control. Theory Appl.* **2023**, *40*, 2104–2129.
6. Kim, C.-S.; Ji, C.-H.; Kim, B.S. Development of a control law to improve the handling qualities for short-range air-to-air combat maneuvers. *Adv. Mech. Eng.* **2020**, *12*, 530–540. [CrossRef]
7. Raivio, T. Capture set computation of an optimally guided missile. *J. Guid. Control. Dyn.* **2001**, *24*, 1167–1175. [CrossRef]
8. Li, S.-Y.; Chen, M.; Wang, Y.-H.; Wu, Q.-X. Air combat decision-making of multiple UCAVs based on constraint strategy games. *Def. Technol.* **2022**, *18*, 368–383. [CrossRef]
9. Park, H.; Lee, B.-Y.; Tahk, M.-J.; Yoo, D.-W. Differential game based air combat maneuver generation using scoring function matrix. *Int. J. Aeronaut. Space Sci.* **2016**, *17*, 204–213. [CrossRef]
10. Virtanen, K.; Karelahti, J.; Raivio, T. Modeling air combat by a moving horizon influence diagram game. *J. Guid. Control. Dyn.* **2006**, *29*, 1080–1091. [CrossRef]
11. Sutton, R.S.; Barto, A.G. Reinforcement Learning: An Introduction. *IEEE Trans. Neural Netw.* **1998**, *9*, 1054. [CrossRef]
12. Ding, D.; Wei, Z.; Tang, S.; Huang, Z. Robust maneuvering decision-making method for air combat using adaptive prediction weight. *Syst. Eng. Electron.* **2020**, *42*, 2275–2284.
13. Ernest, N.; Carroll, D.; Schumacher, C.; Clark, M.; Cohen, K.; Lee, G. Genetic fuzzy based artificial intelligence for unmanned combat aerial vehicle control in simulated air combat missions. *J. Def. Manag.* **2016**, *6*, 1000144. [CrossRef]
14. Ernest, N.D. Genetic Fuzzy Trees for Intelligent Control of Unmanned Combat Aerial Vehicles. Ph.D. Thesis, University of Cincinnati, Cincinnati, OH, USA, 2015.
15. Hu, Z.; Gao, P.; Wang, F. Research on autonomous maneuvering decision of UCAV based on approximate dynamic programming. In Proceedings of the 2019 International Conference on Image and Video Processing, and Artificial Intelligence, Shanghai, China, 23–25 August 2019; SPIE: Bellingham, WA, USA, 2019; pp. 636–641.
16. Tan, M.; Ding, D.; Xie, L.; Ding, W.; Lyu, C. UCAV escape maneuvering decision based on fuzzy expert system and IDE algorithm. *Syst. Eng. Electron.* **2022**, *44*, 1984.
17. Poropudas, J.; Virtanen, K. Analyzing air combat simulation results with dynamic Bayesian networks. In Proceedings of the 2007 Winter Simulation Conference, Washington, DC, USA, 9–12 December 2007; IEEE: Piscataway, NJ, USA, 2007; pp. 1370–1377.
18. Park, S.-J.; Park, S.-S.; Choi, H.-L.; An, K.-S.; Kim, Y.-G. An expert data-driven air combat maneuver model learning approach. In Proceedings of the AIAA Scitech 2021 Forum, Online, 11–21 January 2021; p. 0526.
19. Fu, Y.; Li, C.; Yu, F.R.; Luan, T.H.; Zhang, Y. Hybrid autonomous driving guidance strategy combining deep reinforcement learning and expert system. *IEEE Trans. Intell. Transp. Syst.* **2021**, *23*, 11273–11286. [CrossRef]
20. Silver, D.; Schrittwieser, J.; Simonyan, K.; Antonoglou, I.; Huang, A.; Guez, A.; Hubert, T.; Baker, L.; Lai, M.; Bolton, A. Mastering the game of go without human knowledge. *Nature* **2017**, *550*, 354–359. [CrossRef] [PubMed]
21. Meng, G.; Zhang, H.; Piao, H.; Zhou, M. Cooperative tactical recognition of dual-aircraft formation under incomplete information in BVR air combat. *J. Beijing Univ. Aeronaut. Astronaut.* **2021**, *49*, 284–294.
22. Xing, D.; Zhen, Z.; Gong, H. Offense–defense confrontation decision making for dynamic UAV swarm versus UAV swarm. *Proc. Inst. Mech. Eng. Part G J. Aerosp. Eng.* **2019**, *233*, 5689–5702. [CrossRef]
23. Zhang, H.; Huang, C.; Xuan, Y.; Tang, S. Maneuver decision of autonomous air combat of unmanned combat aerial vehicle based on deep neural network. *Acta Armamentarii* **2020**, *41*, 1613.
24. Hu, J.; Xu, Z.; Wang, W.; Qu, G.; Pang, Y.; Liu, Y. Decentralized graph-based multi-agent reinforcement learning using reward machines. *Neurocomputing* **2024**, *564*, 126974. [CrossRef]
25. Xu, D.; Chen, G. The research on intelligent cooperative combat of UAV cluster with multi-agent reinforcement learning. *Aerosp. Syst.* **2022**, *5*, 107–121. [CrossRef]

26. Zhu, X.; Ai, L. Research on intelligent decision making of many to many unmanned aerial vehicle air combat. *J. Fudan Univ. Nat. Sci.* **2021**, *60*, 410–419.
27. Zhao, R. Research on Intelligent Decision Method for Dual-Aircraft Cooperative Air Combat in Typical Situation. Master's Thesis, Shenyang Aerospace University, Shenyang, China, 2022.
28. Zhao, Y.; Zhang, B.; Xu, A.; Li, H. Two-fighter cooperative tactics maneuvering game and approximate optimal solution. *Syst. Eng. Electron.* **2015**, *37*, 589–593.
29. Wu, A.; Yang, R.; Liang, X.; Zhang, J.; Qi, D.; Wang, N. Visual range maneuver decision of unmanned combat aerial vehicle based on fuzzy reasoning. *Int. J. Fuzzy Syst.* **2022**, *24*, 519–536. [CrossRef]
30. Huang, H.; Dong, K.; Yan, T.; Han, B. Tactical maneuver trajectory optimization for unmanned combat aerial vehicle using improved differential evolution. *Soft Comput.* **2020**, *24*, 5959–5970. [CrossRef]
31. Williams, P. Three-dimensional aircraft terrain-following via real-time optimal control. *J. Guid. Control. Dyn.* **2007**, *30*, 1201–1206. [CrossRef]
32. Hou, Y.; Liang, X.; Zhang, J.; Lv, M.; Yang, A. Hierarchical decision-making framework for multiple UCAVs autonomous confrontation. *IEEE Trans. Veh. Technol.* **2023**, *72*, 13953–13968. [CrossRef]
33. Xie, G.; Gao, H.; Qian, L.; Huang, B.; Li, K.; Wang, J. Vehicle trajectory prediction by integrating physics-and maneuver-based approaches using interactive multiple models. *IEEE Trans. Ind. Electron.* **2017**, *65*, 5999–6008. [CrossRef]
34. Sun, P.; Boukerche, A.; Tao, Y. SSGRU: A novel hybrid stacked GRU-based traffic volume prediction approach in a road network. *Comput. Commun.* **2020**, *160*, 502–511. [CrossRef]
35. Wang, J.; Ding, D.; Chen, C. UCAV trial maneuvering decision under missile attack state assessment. *J. Harbin Inst. Technol.* **2021**, *53*, 118–127.
36. Jitkongchuen, D. A hybrid differential evolution with grey wolf optimizer for continuous global optimization. In Proceedings of the 2015 7th International Conference on Information Technology and Electrical Engineering (ICITEE), Chiang Mai, Thailand, 29–30 October 2015; IEEE: Piscataway, NJ, USA, 2015; pp. 51–54.

Disclaimer/Publisher's Note: The statements, opinions and data contained in all publications are solely those of the individual author(s) and contributor(s) and not of MDPI and/or the editor(s). MDPI and/or the editor(s) disclaim responsibility for any injury to people or property resulting from any ideas, methods, instructions or products referred to in the content.